Tunable 360° Photonic Radio-Frequency Phase Shifter Based on Polarization Modulation and All-Optical Differentiation

Muguang Wang, *Member, IEEE*, and Jianping Yao, *Fellow, IEEE, Fellow, OSA*

***Abstract*—A continuously tunable photonic radio-frequency (RF) phase shifter based on polarization modulation and all-optical differentiation using a polarization modulator (PolM) and an optical frequency discriminator is proposed, theoretically analyzed and experimentally demonstrated. In the proposed phase shifter, two light waves at different wavelengths are injected into a PolM which is driven by an RF signal to be phase shifted. For one wavelength, the state of polarization (SOP) of the light wave is aligned with one principal axis of the PolM, thus the PolM operates jointly with an optical frequency discriminator as an optical differentiator to produce a quadrature (Q) signal. For the other wavelength, the SOP of the light wave is oriented with 45° or 135° with the principal axis of the PolM, thus the PolM operates jointly with a polarizer as an intensity modulator to produce an in-phase (I) signal. By detecting the I-Q optical signals at a photodetector (PD), a phase-shifted RF signal is generated. The value of the phase shift is determined by the amplitudes of the I-Q signals, which can be continuously tuned by controlling the powers of the light waves. An experiment is performed. A phase shifter with a full tunable range of 360° at an RF frequency tunable from 3 to 10 GHz is demonstrated.**

***Index Terms*—All-optical differentiation, frequency discriminator, microwave photonics, polarization modulation, RF phase shifter.**

I. Introduction

THE implementation of photonic radio-frequency (RF) phase shifters has been a topic of research interest in the recent years due to the inherent advantages, such as broad bandwidth and large tunable range, offered by photonics. A wideband phase shifter has many applications such as phased array antennas and broadband wireless communications [1], [2]. Numerous techniques for implementing photonic RF phase shifters have been proposed. In [3]–[6], a photonic RF phase shifter is implemented based on heterodyne mixing of two optical wavelengths, which are generated using a modulator driven by an RF signal with a wavelength spacing corresponding to the frequency of the input RF signal. The phase difference between the two optical wavelengths is introduced by an optical phase shifter. A tunable optical phase shift can be converted to an RF phase shift by heterodyning the two optical wavelengths at a photodetector (PD). Tunable RF phase shift can also be generated based on the nonlinear effects in an optical element such as stimulated Brillouin scattering (SBS) in an optical fiber [7], [8], cross-phase modulation (XPM) and cross-gain modulation (XGM) effects in a semiconductor optical amplifier (SOA) [9], and thermal nonlinear effect in a silicon microring [10]. Recently, photonic RF phase shifters realized based on the slow and fast light effects in an SOA have also been proposed [11], [12], which can also be realized using a tilted fiber Bragg grating (TFBG) [13] or a photonic crystal [14]. Tunable RF phase shift can also be realized based on the vector sum technique, first proposed by Coward *et al.* in [15], in which an in-phase (I) and a quadrature (Q) optical RF signal are generated by injecting an I and a Q RF signal, obtained by using an electrical 90° hybrid coupler, into two Mach-Zehnder modulators (MZMs). By jointly detecting the two optical signals at a PD, a phase shifted RF signal is generated. The RF phase shift is tunable by controlling the amplitudes of the I-Q RF signals through adjusting the optical powers or the bias voltages. The major limitation of the scheme is that two MZMs are needed. The RF signal applied to the two MZMs must be precisely synchronized and thus it is of limited practicality. In addition, a wideband electrical 90° hybrid coupler is needed to achieve the two RF components with quadrature phase, thus the phase shifter is not all-optical but hybrid with limited bandwidth. Several simplified approaches have been proposed to achieve the same phase shifting function using a single MZM [16]–[18]. Two RF components with quadrature phase difference are obtained via an optical differential time delay element connected after the MZM, and the amplitudes of two components are controlled in a complementary way by using a variable directional coupler [16], a polarization controller (PC) [17] or a phase-tunable Mach-Zehnder interferometer [18]. The major limitation of the approaches in [16]–[18] is that the amplitude of the phase-shifted RF signal changes when the phase is tuned. In addition, the phase shift is frequency-dependent or the phase tuning range is not enough to achieve a full 360° phase control, as required by many microwave applications.

In this paper, a novel approach to implementing a continuously tunable photonic RF phase shifter with a full 360° phase

Manuscript received April 09, 2013; accepted June 20, 2013. Date of publication June 27, 2013; date of current version July 10, 2013. This work was supported by the Natural Science and Engineering Research Council of Canada (NSERC). The work of M. Wang was supported by the National Natural Science Foundation of China (NSFC, No. 60807003) and the Program for New Century Excellent Talents in University (NCET, No. NCET-09-0209).

M. Wang is with the Institute of Lightwave Technology, Key Lab of All Optical Network and Advanced Telecommunication Network of EMC, Beijing Jiaotong University, Beijing 100044, China, and also with the Microwave Photonics Research Laboratory, School of Electrical Engineering and Computer Science, University of Ottawa, Ottawa, ON K1N 6N5, Canada (e-mail: mgwang@bjtu.edu.cn).

J. Yao is with the Microwave Photonics Research Laboratory, School of Electrical Engineering and Computer Science, University of Ottawa, Ottawa, ON K1N 6N5, Canada (e-mail: jpyao@eecs.uottawa.ca).

Color versions of one or more of the figures in this paper are available online at http://ieeexplore.ieee.org.

Digital Object Identifier 10.1109/JLT.2013.2271500

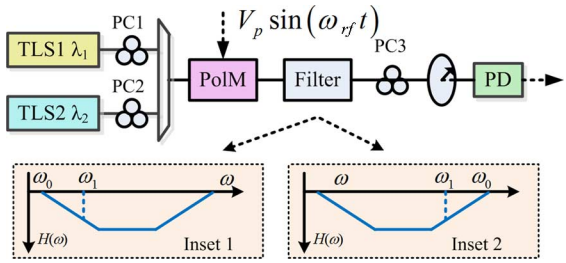

Fig. 1. Schematic of the proposed photonic RF phase shifter using a PolM. TLS: tunable laser source, PC: polarization controller, PolM: polarization modulator, PD: photodetector.

tunable range based on polarization modulation and all-optical differentiation using a polarization modulator (PolM) and an optical frequency discriminator is presented and experimentally demonstrated. In the proposed phase shifter, two light waves at different wavelengths with different states of polarization (SOPs) are injected into a PolM which is driven by an RF signal to be phase shifted. For one wavelength, the SOP is aligned with one principal axis of the PolM, thus the PolM operates jointly with an optical-filter-based frequency discriminator to perform all-optical differentiation, to generate a Q optical signal. For the other wavelength, the SOP is oriented with 45° or 135° with the same principal axis of the PolM, thus the PolM operates jointly with a polarizer to perform equivalently intensity modulation, to generate an I optical signal. When the I-Q optical signals are applied to a PD, a phase-shifted RF signal is generated. The phase of the RF signal is determined by the amplitudes of the I-Q optical signals, and can be tuned continuously by adjusting the optical powers. A full phase tunable range of 360° at an RF frequency tunable from 3 to 10 GHz is experimentally demonstrated.

II. Principle

The schematic of the proposed photonic RF phase shifter is shown in Fig. 1. The key component in the phase shifter is the PolM, which operates as a special phase modulator that can support both TE and TM modes with opposite phase-modulation indices [19]. In the proposed scheme, two light waves from two tunable laser sources (TLSs) at two different wavelengths are multiplexed at a wavelength multiplexer and sent to the PolM through two polarization controllers (PCs), to adjust the SOPs to have an angle of 0° and 45° or 135° to one principal axis of the PolM for λ_1 and λ_2, respectively. An RF signal $V_p \sin(\omega_{rf} t)$ to be phase shifted is modulated on the two light waves at the PolM.

For λ_1, the SOP is controlled to be parallel to the principal axis of the PolM. Thus, the PolM is operating as a phase modulator. An optical filter is connected at the output of the PolM, which functions as a frequency discriminator. The joint operation of the PolM and the optical filter corresponds to an all-optical differentiator, to generate an intensity-modulated Q RF signal. Mathematically, the electrical field of the phase-modulated signal at the output of the PolM is

$$E_{PolM1}(t) = A_1 \exp\left[j\omega_1 t + j\beta \sin(\omega_{rf} t) + j\pi\left(\frac{V_{dc}}{V_\pi}\right)\right] \quad (1)$$

where A_1 and ω_1 are the amplitude and the angular frequency of the optical carrier at λ_1, $\beta = \pi V_p / V_\pi$ is the phase modulation index, and V_π is the half-wave voltage of the PolM and V_{dc} is the bias voltage applied to the PolM. The optical filter as a frequency discriminator has a transfer function with two opposite linear slopes, one of the two slopes can be given by [20]

$$H(\omega) = K(\omega - \omega_0) \quad (2)$$

where K is the slope of the frequency response and ω_0 is an angular frequency on the slope at which $H(\omega) = 0$. When an optical carrier at ω_1 is located at one of the two linear slopes, the filter performs as an all-optical discriminator, and the phase-modulated signal is converted to a differentiated intensity-modulated signal. Thus, a Q signal is generated. The output signal in the frequency domain can be written as

$$E_{f1}(\omega) = K(\omega - \omega_0) E_{PolM1}(\omega) \quad (3)$$

where $E_{PolM1}(\omega)$ is the Fourier transform of $E_{PolM1}(t)$. Applying the inverse Fourier transform to (3), we have the signal in the time domain, given by

$$E_{f1}(t) = [K(\omega_1 - \omega_0) + K\beta\omega_{rf} \cos(\omega_{rf} t)] E_{PolM1}(t) \quad (4)$$

For λ_2, the SOP can be controlled to have an angle of 45° relative to one principal axis of the PolM. Thus, a pair of complementarily phase-modulated signals is generated along the two principal axes of the PolM. The electrical field at the output of the PolM is given by

$$E_{PolM2}(t) = \begin{bmatrix} E_x \\ E_y \end{bmatrix} = \frac{A_2}{\sqrt{2}} \begin{bmatrix} \exp\left[j\omega_2 t + j\beta \sin(\omega_{rf} t) + j\pi\left(\frac{V_{dc}}{V_\pi}\right)\right] \\ \exp\left[j\omega_2 t - j\beta \sin(\omega_{rf} t) - j\pi\left(\frac{V_{dc}}{V_\pi}\right)\right] \end{bmatrix} \quad (5)$$

where A_2 and ω_2 are the amplitude and the angular frequency of the optical carrier at λ_2. Applying the two signals to the optical polarizer with its polarization axis aligned with an angle of 45° with respect to one principal axis of the PolM, a maximal polarization interference will happen and the phase-modulated signals will be combined to generate an intensity-modulated signal, given by

$$E_{pol2} = \frac{\sqrt{2}}{2}(E_x + E_y) = A_2 \exp(j\omega_2 t) \cos\left[\beta \sin(\omega_{rf} t) + \pi\left(\frac{V_{dc}}{V_\pi}\right)\right] \quad (6)$$

It is noted that the optical filter is transparent to λ_2 and has no impact on the output at λ_2. For the optical carrier at λ_1, the SOP of the signal has an angle of 45° with respect to the polarization axis of the optical polarizer. Thus, the optical field at output of the optical polarizer is given by

$$E_{pol1} = E_{f1}(t) \cos\left(\frac{\pi}{4}\right) \quad (7)$$

Since the two light waves are generated by two independent light sources with different wavelengths, at the frequency of ω_{rf}, the photocurrent at the output of the PD is the sum of the photocurrents produced by the two optical signals at λ_1 and λ_2. It can be written as

$$i_{pd} = i_{pd1} + i_{pd2} \tag{8}$$

where i_{pd1} and i_{pd2} are given by

$$i_{pd1} = RK^2 I_1 (\omega_1 - \omega_0)\, \beta \omega_{rf} \cos(\omega_{rf} t) \tag{9.1}$$

$$i_{pd2} = RI_2 J_1(2\beta) \cos\left[2\pi\left(\frac{V_{dc}}{V_\pi}\right) + \frac{\pi}{2}\right] \sin(\omega_{rf} t) \tag{9.2}$$

where R is the responsivity of the PD, $J_1(2\beta)$ is the first-order Bessel function of the first kind, and $I_{1(2)}$ is the optical power output from the $\mathrm{TLS}_{1(2)}$. It can be seen from (9) that the two RF signal are quadrature in phase. Let

$$a = RK^2 I_1 (\omega_1 - \omega_0)\, \beta \omega_{rf} \tag{10.1}$$

$$b = RI_2 J_1(2\beta) \cos\left[2\pi\left(\frac{V_{dc}}{V_\pi}\right) + \frac{\pi}{2}\right] \tag{10.2}$$

The photocurrent at the frequency of ω_{rf} can be rewritten as

$$i_{pd} = a\cos(\omega_{rf} t) + b\sin(\omega_{rf} t) = i_p \sin(\omega_{rf} t + \theta) \tag{11}$$

where i_p and θ are the amplitude and the phase shift of the RF signal, and can be expressed as

$$i_p = \sqrt{a^2 + b^2} \tag{12.1}$$

$$\theta = \arctan\left(\frac{a}{b}\right) \tag{12.2}$$

It can be seen that the phase shift of the RF signal can be easily tuned by tuning the coefficients a and b. The RF signal can also be expressed in a complex form, given by

$$z = b + ja = i_p \exp(j\theta) \tag{13}$$

Note that if the coefficients, a and b, are all positive, from a theoretical point of view, the tunable range of the phase shift would only be 0~90°. However, from (10.1) it can be seen that the coefficient, a, can be either positive or negative by locating the optical carrier ω_1 at either the left or the right slope of the frequency response of the optical filter, as shown in the insets of Fig. 1. When the optical carrier at ω_1 is located at the falling edge of the filter frequency response, that is, $\omega_1 - \omega_0 > 0$, the coefficient, a, would be positive. The coefficient, a, would be negative when the optical carrier at ω_1 is located at the rising edge of the frequency response of the optical filter. While for coefficient b, it can be seen from (10.2) that it can also be positive or negative depending on the bias voltage V_{dc}, without affecting the coefficient a. In addition, it should be noted that the sign of coefficient b can also be changed by adjusting the input SOP of λ_2 at an angle of 45° or 135° relative to one principal axis of the PolM. Thus, a tunable phase shift with a full 360° phase tunable range can be achieved which covers all the four quadrants in the complex plane.

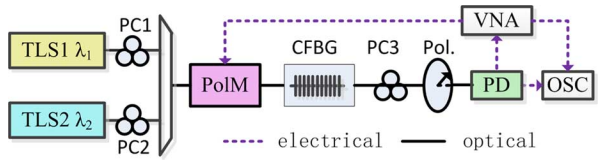

Fig. 2. Experimental setup of the proposed RF phase shifter. TLS: tunable laser source, PC: polarization controller, PolM: polarization modulator, CFBG, chirped fiber Bragg grating, Pol.: polarizer, VNA: vector network analyzer, PD: photodetector, OSC: oscilloscope.

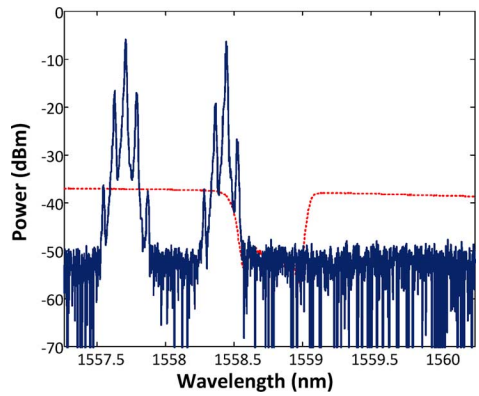

Fig. 3. Spectra of the CFBG and two optical signals with one located at the left slope of the spectrum of the CFBG.

III. Experimental Setup

The proposed photonic RF phase shifter is experimentally demonstrated. Fig. 2 shows the experimental setup. Two light waves at λ_1 and λ_2 from two TLSs (Agilent N7714A) are sent to a PolM via two PCs and a 2 × 1 coupler. The PCs are used to adjust the SOPs of the two light waves, to make them aligned with an angle of $\theta_1 = 0°$ and $\theta_2 = 45°$ or 135° relative to one principal axis of the PolM. The PolM used in the experiment is an AlGaAs-GaAs 40-Gb/s mode-converter-based modulator from Versawave Technologies. A RF tone generated by a vector network analyzer (VNA, Agilent E8364A) is applied to the PolM via the RF port to modulate the light waves. For λ_1, the PolM operates as a phase modulator. The joint operation of the PolM and a frequency discriminator corresponds to an optical differentiator to produce a Q optical signal. The frequency discriminator in the proposed system is realized using a chirped fiber Bragg grating (CFBG). For λ_2, since the SOP is adjusted to have an angle of 45° or 135° relative to one principal axis, the PolM operates as a polarization modulator. The joint operation of the PolM and a polarizer corresponds to as an intensity modulator to produce an I optical signal.

The transmission spectrum of the CFBG is measured by using an erbium-doped fiber amplifier (EDFA) as a broadband optical source, while the optical spectrum of two light waves modulated by an RF frequency at 10 GHz is measured at the output of the CFBG. Fig. 3 shows the corresponding results monitored by an optical spectrum analyzer (OSA, Ando AQ6317B). For λ_1 at 1558.442 nm, it can be seen that RF-modulated optical signal is located at the left slope of the transmission spectrum of the CFBG, and the phase-modulated signal is converted into an intensity-modulated signal at the output of the CFBG. As

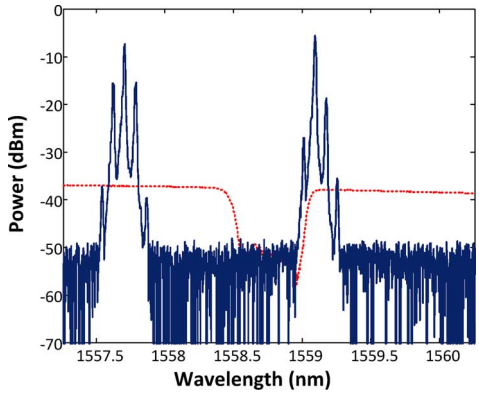

Fig. 4. Spectra of the CFBG and two optical signals with one located at the right slope of the CFBG.

expected, the power of the right sideband of the signal is about 10 dB lower than that of the left sideband. While the CFBG is transparent to the other light wave λ_2 for that the wavelength of 1557.698 nm is far away from the stop band of the CFBG. A polarizer is connected after the CFBG with its polarization axis aligned with an angle of 45° to one principal axis of the PolM by a third PC (PC3). At the polarizer, for λ_2 at 1557.698 nm, two orthogonally polarized components would interfere, and an intensity-modulated RF optical signal is obtained. While for the RF optical signal of λ_1 at 1558.442 nm, there would be a 3 dB loss without any shape distortion because its SOP is aligned with an angle of 45° relative to the principle axis of the polarizer. Thus, an I and a Q RF-modulated optical signals are then generated which are summed up at the PD, with the combined electrical waveform observed by a sampling oscilloscope (OSC, Agilent 86100C).

To fulfil a tunable range of 0~360°, it is necessary to switch the wavelength of the first light wave from one slope of the CFBG to the other slope, to obtain a positive and negative coefficient of a, given in (10). Fig. 4 shows the optical spectrum of the 10 GHz RF-modulated signal when the optical carrier λ_1 is at 1559.096 nm, located at the right slope of the transmission spectrum of the CFBG. Compared with Fig. 3, as can be seen the power of the right sideband of the signal is about 10 dB higher than that of the left sideband.

IV. Results and Discussion

The tunable range of the RF phase shifter is investigated. As shown in (10)–(12), the tuning of the phase shift can be done by adjusting the coefficients (a, b). First, the input SOP of the light wave from TLS2 is adjusted to have an angle of 45° relative to one principal axis of the PolM, and the light wave from TLS1 have a wavelength of 1558.442 nm located at the left slope of the CFBG. We use the OSC to monitor the output phase-shifted RF signal. When the phase is tuned, the RF signal is laterally shifted. Fig. 5 shows the waveforms of the phase-shifted RF signal at 10 GHz. The phase-shifted RF signal for $(a, b) = (0, 1)$ is chosen as a reference. Note that to maintain a constant power of the phase-shifted RF signal, the coefficients are normalized to satisfy $\sqrt{a^2 + b^2} = 1$.

The phase shift tuning is performed by weighting the two coefficients a and b while maintaining $\sqrt{a^2 + b^2} = 1$, realized by

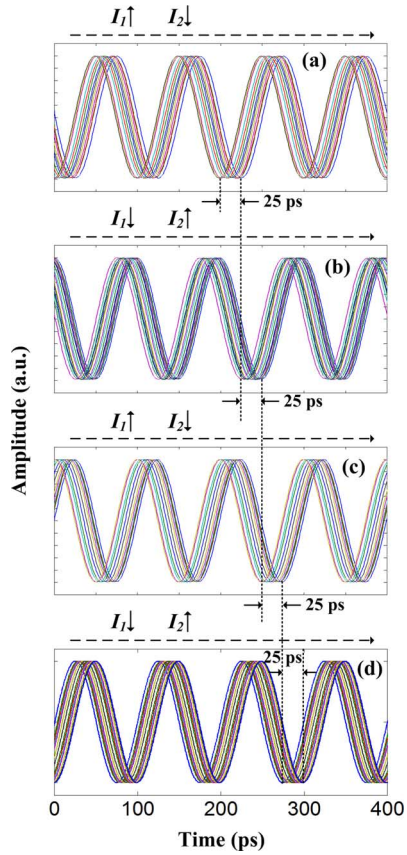

Fig. 5. Phase-shifted RF signals at 10 GHz with different phase shifts. (a) $\lambda_1 = 1558.442$ nm, $\theta_1 = 0°$, $\theta_2 = 45°$, (b) $\lambda_1 = 1558.442$ nm, $\theta_1 = 0°$, $\theta_2 = 135°$, (c) $\lambda_1 = 1559.096$ nm, $\theta_1 = 0°$, $\theta_2 = 135°$, (d) $\lambda_1 = 1559.096$ nm, $\theta_1 = 0°$, $\theta_2 = 45°$.

adjusting the output optical powers I_1 and I_2 of the two TLSs. Note that the coefficient, b, can also be controlled by adjusting the bias voltage of the PolM according to (10). It can be seen from Fig. 5(a) the RF signal at the output of the PD is laterally delayed from 0 to 25 ps, i.e., a tunable phase shift from 0° to 90°. The phase tunable process can also be shown in the complex plane according to (13). In this case, a and b are both positive, and are from (0, 1) to (1, 0) corresponding to the first quadrant of the complex plane, as shown in Fig. 6, where the dark dots on the unit circle represent the corresponding waveforms shown in Fig. 5(a).

To increase the tunable range, the SOP of the light wave from TLS2 is adjusted to have an angle of 135° to one principal axis of the PolM. Then, a delay of the waveforms from 25 to 50 ps, i.e., a tunable phase shift of the RF signals from 90° to 180°, is achieved by adjusting the output optical powers I_1 and I_2. The phase shifted RF signal is shown in Fig. 5(b). In this case, the coefficients (a, b) are tuned from $(0, -1)$ to $(1, 0)$, corresponding to a phase in the second quadrant of the complex plane as shown in Fig. 6, where the red dots on the unit circle represent the corresponding waveforms shown in Fig. 5(b). The tunable range can also be increased by locating the wavelength of the light wave from TLS1 at the right slope of the CFBG. Then, a delay of the waveforms is from 50 to 75 ps, i.e., a tunable phase shift from 180 to 270° is achieved. The phase-shifted RF signal is shown in Fig. 5(c). In this case, the coefficients (a, b) are tuned from

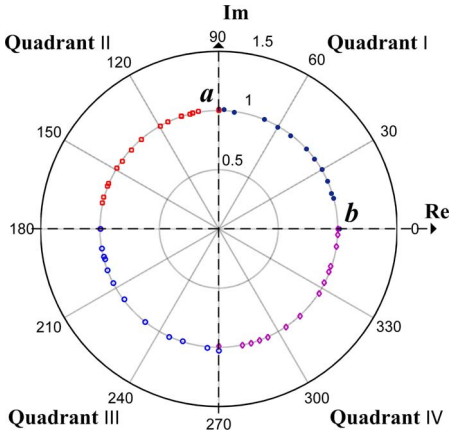

Fig. 6. Measured relative phase shift by weighting coefficients (a, b) in a complex plane.

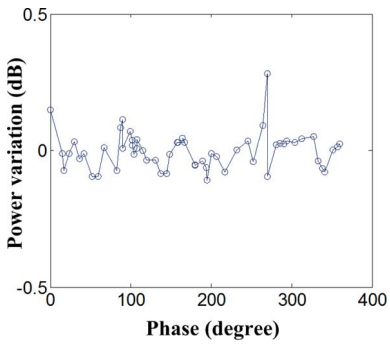

Fig. 7. Measured power variations in the full 360° tunable range.

$(0, -1)$ to $(-1, 0)$, corresponding to a phase in the third quadrant of the complex plane, as shown in Fig. 6, where the blue dots on the unit circle represent the corresponding waveforms shown in Fig. 5(c). In addition, by switching the SOP of the light wave from TLS2 back from 135° to 45°, a delay of the waveforms from 75 to 100 ps, i.e., a tunable phase shift from 270 to 360° would be achieved. Fig. 5(d) shows the corresponding RF signal. In this case, the coefficients (a, b) are tuned from $(-1, 0)$ to $(0, 1)$, corresponding to a phase in the fourth quadrant of the complex plane, as shown in Fig. 6, where the pink dots on the unit circle represent the corresponding waveforms shown in Fig. 5(d). Thus, by reconfiguring the phase shifter, a continuously tunable phase shift with a full tunable range of 360° is demonstrated.

It is desirable that the output power of the phase shifted RF signal is maintained constant when the phase is being tuned. During the tuning process, since the condition $\sqrt{a^2 + b^2} = 1$ is always satisfied, the power of the RF signal should be maintained constant. This is verified by measuring the power of the phase-shifted RF signal during the tuning. Fig. 7 shows the relative power variations. As can be seen the power variations when the phase is tuned in the full 360° tunable range are very small, less than 0.3 dB.

The phase response of the proposed phase shifter over a frequency range from 3 to 10 GHz is also measured, which is done using the VNA. In the measurement process, the tuning is performed by adjusting the DC bias voltage of the PolM. Specifically, the DC bias voltage to the PolM is tuned from 4 to 17.77 V, corresponding to a literal shift of the transfer function of the PolM by about half-wave period, and the wavelength of the light wave from TLS1 is set at 1558.442 nm and 1559.496 nm successively, corresponding to the tunable range for the lower $-180 \sim 0°$ and upper $0 \sim 180°$, respectively, as shown in Fig. 8. It can be seen that the phase response of the proposed phase shifter is almost constant over a large frequency range, which is highly expected for broadband applications.

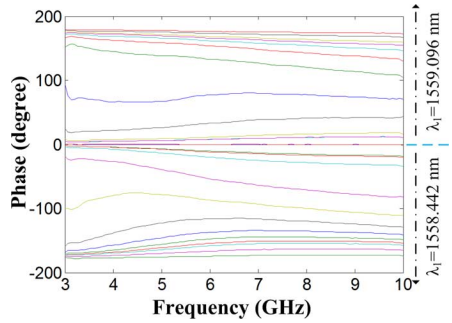

Fig. 8. Frequency response of the photonic RF phase shifter with different phase shift.

V. Conclusion

We have proposed and experimentally demonstrated a novel approach to implementing a continuously tunable photonic RF phase shifter with a full tunable range of 360° based on the polarization modulation and all-optical differentiation. An experiment was performed, in which two light waves at different wavelengths with different SOPs were sent to a PolM which was driven by the RF signal to be phase shifted. For one wavelength, the PolM was operating with a CFBG as a frequency discriminator to realize an all-optical differentiation and produce a Q optical signal. For the other wavelength, the PolM was operating with a polarizer to perform equivalent intensity modulation and produce an I optical signal. By detecting the I-Q optical signals at the PD, a phase-shifted RF signal was generated. The tuning of the phase shift was simply implemented by tuning the optical powers of the two optical sources. A phase shifter with a tunable range of 360° at an RF frequency tunable from 3 to 10 GHz was demonstrated. The power of the phase-shifted RF signal was maintained constant with slight variations of less than 0.3 dB over the full tunable range of 360°.

References

[1] J. P. Yao, "Microwave photonics," *J. Lightw. Technol.*, vol. 27, no. 3, pp. 314–335, Feb. 2009.

[2] J. Capmany, B. Ortega, D. Pastor, and S. Sales, "Discrete-time optical processing of microwave signals," *J. Lightw. Technol.*, vol. 23, no. 2, pp. 702–723, Feb. 2005.

[3] S. S. Lee, A. H. Udupa, H. Erlig, H. Zhang, Y. Chang, C. Zhang, D. H. Chang, D. Bhattacharya, B. Tsap, W. H. Steier, L. R. Dalton, and H. R. Fetterman, "Demonstration of a photonically controlled RF phase shifter," *IEEE Microw. Guided Wave Lett.*, vol. 9, no. 9, pp. 357–359, Sep. 1999.

[4] J. Han, H. Erlig, D. Chang, M. C. Oh, H. Zhang, C. Zhang, W. Steier, and H. Fetterman, "Multiple output photonic RF phase shifter using a novel polymer technology," *IEEE Photon. Technol. Lett.*, vol. 14, no. 4, pp. 531–533, Apr. 2002.

[5] Z. H. Li, C. Y. Yu, Y. Dong, L. H. Cheng, L. F. K. Lui, C. Lu, A. P. T. Lau, H. Y. Tam, and P. K. A. Wai, "Linear photonic radio frequency phase shifter using a differential-group-delay element and an optical phase modulator," *Opt. Lett.*, vol. 35, no. 11, pp. 1881–1883, Jun. 2010.
[6] W. Zhang and J. P. Yao, "Photonic generation of millimeter-wave signals with tunable phase shift," *IEEE Photon. J.*, vol. 4, no. 3, pp. 889–894, Jun. 2012.
[7] A. Loayssa and F. J. Lahoz, "Broad-band RF photonic phase shifter based on stimulated Brillouin scattering and single-sideband modulation," *IEEE Photon. Technol. Lett.*, vol. 18, no. 1, pp. 208–210, Jan. 2006.
[8] W. Li, N. H. Zhu, and L. X. Wang, "Photonic phase shifter based on wavelength dependence of Brillouin frequency shift," *IEEE Photon. Technol. Lett.*, vol. 23, no. 14, pp. 1013–1015, Jul. 2011.
[9] X. Li, Y. Yu, J. J. Dong, and X. L. Zhang, "Widely tunable microwave photonic filter based on semiconductor optical amplifier," *Proc. SPIE*, vol. 7988, pp. 201–206, 2011.
[10] Q. J. Chang, Q. Li, Z. Y. Zhang, M. Qiu, T. Ye, and Y. K. Su, "A tunable broadband photonic RF phase shifter based on a silicon microring resonator," *IEEE Photon. Technol. Lett.*, vol. 21, no. 1, pp. 60–62, Jan. 2009.
[11] W. Q. Xue, S. Sales, J. Capmany, and J. Mork, "Microwave phase shifter with controllable power response based on slow- and fast-light effects in semiconductor optical amplifiers," *Opt. Lett.*, vol. 34, no. 7, pp. 929–931, Apr. 2009.
[12] J. Sancho, J. Lloret, I. Gasulla, S. Sales, and J. Capmany, "Fully tunable 360 degrees microwave photonic phase shifter based on a single semiconductor optical amplifier," *Opt. Exp.*, vol. 19, no. 18, pp. 17421–17426, Aug. 2011.
[13] H. Shahoei and J. P. Yao, "Tunable microwave photonic phase shifter based on slow and fast light effects in a tilted fiber Bragg grating," *Opt. Exp.*, vol. 20, no. 13, pp. 14009–14014, Jun. 2012.
[14] T. Baba, "Slow light in photonic crystals," *Nature Photon.*, vol. 2, no. 8, pp. 465–473, Aug. 2008.
[15] J. F. Coward, T. K. Yee, C. H. Chalfant, and P. H. Chang, "A photonic integrated-optic RF phase-shifter for phased-array antenna beam-forming applications," *J. Lightw. Technol.*, vol. 11, no. 12, pp. 2201–2205, Dec. 1993.
[16] L. A. Bui, A. Mitchell, K. Ghorbani, and T. H. Chio, "Wideband RF photonic vector sum phase-shifter," *Electron. Lett.*, vol. 39, no. 6, pp. 536–537, Mar. 2003.
[17] K. H. Lee, Y. M. Jhon, and W. Y. Choi, "Photonic phase shifters based on a vector-sum technique with polarization-maintaining fibers," *Opt. Lett.*, vol. 30, no. 7, pp. 702–704, Apr. 2005.
[18] X. X. Xue, X. P. Zheng, H. Y. Zhang, and B. K. Zhou, "Tunable 360 degrees photonic radio frequency phase shifter based on optical quadrature double-sideband modulation and differential detection," *Opt. Lett.*, vol. 36, no. 23, pp. 4641–4643, Dec. 2011.
[19] J. D. Bull, N. A. F. Jaeger, H. Kato, M. Fairburn, A. Reid, and P. Ghanipour, "40-GHz electro-optic polarization modulator for fiber optic communications systems," *Photonics North 2004: Opt. Compon. Devices*, vol. 5577, pp. 133–143, Sep. 2004.
[20] J. P. Yao, "Photonics for ultrawideband communications," *IEEE Microw. Mag.*, vol. 10, no. 4, pp. 82–95, Jun. 2009.

Muguang Wang received the B.S. degree in optics from Shandong University, Jinan, China in 1999, and the Ph.D. degree in electrical engineering from Beijing Jiaotong University, Beijing, China in 2004.

In 2004, he joined the Institute of Lightwave Technology, Key Lab of All Optical Network & Advanced Telecommunication Network of EMC, Beijing Jiaotong University, Beijing, China, as a Lecturer, where he has been an Associate Professor since 2006. He is currently a visiting researcher in the Microwave Photonics Research Laboratory, School of Electrical Engineering and Computer Science, University of Ottawa, Ontario, Canada. His current research interests include optical fiber communications and networking, microwave photonics, and optical signal processing.

Jianping Yao (M'99–SM'01–F'12) received the Ph.D. degree in electrical engineering from the Université de Toulon, Toulon, France, in December 1997. He joined the School of Electrical Engineering and Computer Science, University of Ottawa, Ottawa, Ontario, Canada, as an Assistant Professor in 2001, where he became an Associate Professor in 2003, and a Full Professor in 2006. He was appointed University Research Chair in Microwave Photonics in 2007. From July 2007 to June 2010, he was the Director of the Ottawa-Carleton Institute for Electrical and Computer Engineering. Prior to joining the University of Ottawa, he was an Assistant Professor in the School of Electrical and Electronic Engineering, Nanyang Technological University, Singapore, from 1999 to 2011. Prof. Yao is a principal investigator of more than 20 projects, including five strategic grant projects funded by the Natural Sciences and Engineering Research Council of Canada. He has published more than 410 papers, including more than 230 papers in peer-reviewed journals and 180 papers in conference proceedings.

His research interests focus on microwave photonics, which includes photonic processing of microwave signals, photonic generation of microwave, millimeter-wave and terahertz, radio over fiber, ultrawideband over fiber, and photonic generation of microwave arbitrary waveforms. His research also covers fiber optics and biophotonics, which includes fiber lasers, fiber and waveguide Bragg gratings, fiber-optic sensors, microfluidics, optical coherence tomography, and Fourier-transform spectroscopy. Dr. Yao is currently an Associate Editor of the International Journal of Microwave and Optical Technology. He is on the Editorial Board of the IEEE Transactions on Microwave Theory and Techniques. He is a Chair of numerous international conferences, symposia, and workshops, including the Vice Technical Program Committee (TPC) Chair of the IEEE Microwave Photonics Conference in 2007, the TPC Co-Chair of the Asia-Pacific Microwave Photonics Conference in 2009 and 2010, the TPC Chair of the high-speed and broadband wireless technologies subcommittee of the IEEE Radio Wireless Symposium in 2009–2012, the TPC Chair of the microwave photonics subcommittee of the IEEE Photonics Society Annual Meeting in 2009, the TPC Chair of the IEEE Microwave Photonics Conference in 2010, and the General Co-Chair of the IEEE Microwave Photonics Conference in 2011. He is also a committee member of numerous international conferences. Prof. Yao received the 2005 International Creative Research Award at the University of Ottawa. He was the recipient of the 2007 George S. Glinski Award for Excellence in Research and an inaugural OSA Outstanding Reviewer Award in 2012. Currently, Prof. Yao serves as an IEEE Distinguished Microwave Lecturer for 2013–2015.

Prof. Yao is a registered Professional Engineer of Ontario. He is a Fellow of IEEE, a Fellow of the Optical Society of America (OSA), and a Fellow of the Canadian Academy of Engineering (CAE).